From the printer to the lungs: Inkjet-printed aerogel particles for pulmonary delivery

Clara López-Iglesias, Alba M. Casielles, Ayça Altay, Ruggero Bettini, Carmen Alvarez-Lorenzo, Carlos A. García-González

PII: S1385-8947(18)31873-4
DOI: https://doi.org/10.1016/j.cej.2018.09.159
Reference: CEJ 19998

To appear in: *Chemical Engineering Journal*

Received Date: 22 May 2018
Revised Date: 18 September 2018
Accepted Date: 20 September 2018

Please cite this article as: C. López-Iglesias, A.M. Casielles, A. Altay, R. Bettini, C. Alvarez-Lorenzo, C.A. García-González, From the printer to the lungs: Inkjet-printed aerogel particles for pulmonary delivery, *Chemical Engineering Journal* (2018), doi: https://doi.org/10.1016/j.cej.2018.09.159

From the printer to the lungs: Inkjet-printed aerogel particles for pulmonary delivery

Clara López-Iglesias[a], Alba M. Casielles[a], Ayça Altay[b], Ruggero Bettini[b], Carmen Alvarez-Lorenzo[a], Carlos A. García-González[a,*]

[a]*Departamento de Farmacología, Farmacia y Tecnología Farmacéutica, R+D Pharma group (GI-1645), Facultad de Farmacia and Health Research Institute of Santiago de Compostela (IDIS), Universidade de Santiago de Compostela, E-15782-Santiago de Compostela, Spain*

[b]*Food and Drug Department, University of Parma, Parco Area delle Scienze 27/A, 43124 Parma, Italy*

[*]*Corresponding author:* carlos.garcia@usc.es; *phone: +34 881 815252; fax: +34 981 547148.*

Declarations of interest: none

Abstract

Inkjet printing is as an emerging technique in the biomedical field offering cost-effective solutions for flexible production and the engineering of personalized medicine solutions. Thermal inkjet printing technology in the "drop-on-demand" mode allows the design of fully automated deposition patterns with high spatial resolution for applications ranging from microparticles in drug formulations to cell deposition in regenerative medicine. In particular, novel formulations in the form of porous particles are sought for the treatment of respiratory disorders and the systemic administration of bioactive compounds using the pulmonary route. Aerogel particles, i.e. highly porous and light-weight nanoporous powders, are particularly promising as carriers for the pulmonary route. In this work, the preparation of aerogel microspheres by thermal inkjet printing followed by supercritical drying is presented for the first time to overcome the current processing limitations. Alginate aerogel particles were loaded with salbutamol sulphate, a bronchodilator used for the treatment of asthma attacks and chronic obstructive pulmonary disease, as a model drug for sustained pulmonary delivery. The optimized processing method allowed the preparation of reproducible nanostructured

microparticles with modified salbutamol sulphate release profile and aerodynamic performance of relevance for oral inhalation purposes.

Keywords: aerogel; supercritical drying; salbutamol sulphate; inkjet printing

1. Introduction

Inkjet printing has emerged as a relevant technique for several applications like electronic devices, photoelectrochemical cells or drug products [1-3]. "Drop on demand" is a particular approach of this technique for the pharmaceutical and biomedical sector to address the current challenges in cost-effective research, scalability, supply chain, flexible production and personalized medicine [3, 4]. This technology is also commercially available for 3D-bioprinting with high cell viabilities (above 85%) [5, 6]. Thermal inkjet printing in the "drop on demand" mode is a promising technology that allows the versatile and digitally-controlled secondary processing of pharmaceuticals as printed particles for drug delivery systems with repeatability, narrow particle size distribution and high spatial resolution. Using this method, droplet volumes of *ca.* 1-70 pL are ejected from small nozzles due to the expansion of a vapor bubble produced by electrical heating of the liquid itself [4, 7]. The resulting ejected droplet has a diameter close to that of the nozzle itself (10-50 μm). Several inkjet-printed pharmaceutical formulations in the form of particles, hydrogels and films were reported for different administration routes (e.g., oral, respiratory or parenteral) [3, 4, 8-11].

For pulmonary delivery, novel formulations in the form of dry powder are sought for the treatment of respiratory disorders and the systemic delivery of bioactive compounds to maximize their therapeutic effect resulting in lower doses and reduced public health costs [12]. For these purposes, dry powder formed by particles of aerodynamic diameters targeting 1-5 μm are being developed with optimum aerodynamic particle size distribution (APSD) for penetration to the deep lung. The production of large porous particles with geometric diameters greater than 5 μm preserving the target APSD is desired. The tendency for aggregation of these porous particles is much lower than that of their non-porous counterparts due to their lower densities and larger diameters [12].

Aerogel particles are highly porous, light-weight powders of particular interest as carriers for the pulmonary route [13-15]. Proteins and polysaccharide aerogels are biocompatible, biodegradable mesoporous carriers with high loading capacities for bioactive compounds [16-19]. The use of these nanostructured materials in the form of microspheres would result in uniform particle dispersion and a subsequent more reliable therapeutic effect. Several approaches have been proposed for the engineering of the aerogel design in terms of morphology, mechanical strength and composition [13, 14, 20-22]. In spite of the recent advances in "aerogel engineering", the biomedical applications of aerogel processing are still constrained by the difficulty of controlling simultaneously the aerogel particle size and morphology and the release pattern of the loaded bioactive compounds. Current techniques for pulmonary delivery are constrained in terms of particle size (prilling [23], jet cutting [24]), control of particle size distribution (jet milling [25]) or the presence of surfactants (gel-emulsification [26, 27]). Overall, no surfactant-free aerogel microspheres with a relevant particle size for pulmonary administration have been reported so far in the literature.

The combination of thermal inkjet printing and aerogel technology is an auspicious engineering solution to obtain nanostructured porous microspheres with narrow particle size distribution for oral inhalation. Excipient-free drug particles of 3-20 μm diameter with pore gradient in the micron-size range were previously obtained by thermal inkjet spray-freeze drying [28, 29]. Silica aerogels of 0.1-1.0 μm diameter were prepared using thermal inkjet printing gel-emulsification [30]. To the best of our knowledge, preparation by thermal inkjet printing of aerogel particles with pores in the nano-size range and aerodynamic particle sizes suitable for its use as carriers for oral inhalation has not been reported before.

In this work, a protocol for the preparation of alginate aerogel microspheres by inkjet printing followed by supercritical drying is presented for the first time. Choice of alginate as aerogel source is of relevance since derivatives of this polysaccharide have proven to promote the mucus fluidity and clearance of sputum in Phase 2a clinical trials for the cystic fibrosis treatment [31, 32]. Aerogel particles were loaded with salbutamol sulphate, a bronchodilator used for the treatment of asthma and chronic obstructive pulmonary disease. Particles were

evaluated regarding their textural, morphological and aerodynamic properties and the drug release tested in a relevant medium for the respiratory route.

2. Materials and methods

2.1 Materials

Alginic acid sodium salt from brown algae, (guluronic acid/mannuronic acid ratio of 70/30, M_w 403 kDa) was obtained from Sigma Aldrich (Irvine, UK). Salbutamol sulphate (SS, M_w 337.4 g/mol, >99% purity) and calcium chloride dihydrate ($CaCl_2 \cdot 2H_2O$) were provided by Fagron Ibérica (Terrassa, Spain) and Merck (Darmstadt, Germany), respectively. Carbon dioxide (CO_2, >99.8% purity) was supplied by Praxair, Inc. (Madrid, Spain). Phosphate buffer solution (PBS) pH 7.4 and 7.0 was used in the release and aerodynamic tests, respectively, and prepared using sodium hydroxide (NaOH, 99% purity) and potassium dihydrogen phosphate (>99.5 % purity) purchased from VWR International (Geldenaaksebaan, Belgium). Absolute-grade ethanol from Merck (Darmstadt, Germany), methanol (VWR International, Milan, Italy) and water purified using reverse osmosis (resistivity > 18 MΩ·cm, MilliQ, Millipore®, Spain) were also used.

2.2 Preparation of alginate aerogel beads by prilling

Aqueous alginate solutions of varied concentrations (0.25, 0.5, 0.75, 1.0, 1.25 and 1.5 % (w/w)) were prepared by mechanical stirring (600 rpm) at room temperature for 15 min. After settling for *ca.* 4 h to remove the air bubbles within the solution, 10 mL of the alginate solutions were added dropwise to 100 mL of 0.5 M $CaCl_2$ aqueous solution and at a flow rate of 5 mL/min by using a syringe pump (AL-1000, World Precision Instruments, Sarasota, FL, USA) with a nozzle diameter of 2.0 mm. Alginate gel beads were immediately formed when in contact with the gelation bath. The gel beads were collected after 5 h of ageing and subjected to either a direct or sequential (ethanol:water volume ratio 0:100, 50:50, 75:25, 100:0 (x2)) solvent exchange to ethanol. The gel beads were placed into paper cartridges and put into the 100-mL extractor vessel of the high pressure equipment used (Waters-Thar Process, Pittsburg, PA, USA). Finally, a flow of 5 g/min of supercritical CO_2 (40 ºC, 120 bar) passed through the pressurized vessel containing the gel particles and extracted the liquid EtOH contained in the

gels whilst preserving their original polymer network [33]. After 3.5 h of drying, alginate aerogel particles were obtained.

2.3 Preparation of aerogel microspheres prepared by inkjet printing

Aqueous alginate solutions of varied concentrations (0.25, 0.30, 0.35, 0.40 % (w/w)) were prepared as above. 10 mL of the alginate solutions were loaded in the cartridges (HP51626A) of a thermal inkjet printer (Hewlett Packard Deskjet 340, Palo Alto, CA, USA). The inkjet printer was previously modified by removing its external cover and mounting it into a support allowing the control of the height of the device (Fig. 1). The alginate-based ink was printed over a borosilicate dish (internal diameter: 6.2 cm) containing 25 or 100 mL of $CaCl_2$ 0.5 M solution as gelation bath. This bath was located 4 cm below the printhead and magnetically stirred at 300 rpm. The inkjet printing was carried out at the standard speed, in a 24.7 x 3.6 cm^2 rectangular region and using 30 or 120 printing cycles depending on the volume (25 or 100 mL) of the gelation bath. The gel beads were collected in a Falcon tube, left 5 h for ageing and then subjected to either a direct (twice) or sequential (ethanol:water volume ratio 0:100, 50:50, 75:25, 100:0 (x2)) solvent exchange to ethanol. Finally, alginate alcogel microspheres were filled in paper cartridges and dried under a continuous flow of supercritical CO_2 (40 ºC, 120 bar, 5 g $CO_2 \cdot min^{-1}$, 3.5 h) to obtain the corresponding aerogels (*cf.* Section 2.2).

FIGURE 1

2.4 Preparation of salbutamol-loaded aerogel microspheres prepared by inkjet printing

For the preparation of salbutamol-loaded aerogels, the same printing procedure as the one reported in Section 2.3 was employed but the drug was added at a concentration of 0.35 % (w/w) to 25 mL of the gelation bath of $CaCl_2$ solution. A direct solvent exchange of the gel microspheres to ethanol (twice) was used in this case before undergoing the supercritical drying.

2.5 Structural and physicochemical characterization of the gels and aerogels

Images from the external morphology of the printed aerogels were obtained by scanning electron microscopy (SEM, EVO LS15, Zeiss, Oberkochen, Germany). Samples were iridium-sputtered (10 nm thickness) prior to imaging to minimize charging and to improve the contrast of the images. Focused Ion Beam technique (Dual Beam Helios Nanolab 600, FEI, Hillsboro,

OR, USA) coupled with SEM microscopy (FIB-SEM) was used to obtain the images of the internal morphology of the printed aerogels from cross sections of the microspheres. A milling with Ga^+ ions (26 pA, 30 kV) was performed for the automated FIB-SEM slice-and-view method used.

Textural properties of the aerogels were characterized using low-temperature N_2 adsorption–desorption analysis (ASAP 2000; Micromeritics Inc.; Norcross, GA, USA). Before the measurements, the aerogel powder was dried under vacuum (<1 mPa) at room temperature for 24 h. Specific surface area (A_{BET}) was calculated applying the BET (Brunauer–Emmett–Teller) method. The BJH (Barrett–Joyner–Halenda) method was used to estimate the specific pore volume ($V_{p,BJH}$) and the mean pore diameter ($d_{p,BJH}$).

Overall porosity (ε) was calculated using Eq. (1), where ρ_{bulk} is the bulk density estimated from the tapped density (*ca.* 1.26-fold the tapped density [34]) and ρ_{skel} is the skeletal density of the alginate particles measured from five replicates by helium pycnometry (Quantachrome; Boynton Beach, FL, USA) at 25 ºC and 1.03 bar. Tapped density (ρ_{tapped}) was calculated with the graduated flask method from three replicates of the volume occupied by a certain weight of tapped aerogel particles.

$$\varepsilon = \left(1 - \rho_{bulk}/\rho_{skel}\right) \cdot 100 \quad (1)$$

The mass median aerodynamic diameter of the pristine aerogel particles (d_{aero}) was obtained from the simplification of Stokes' law for particles with diameters higher than 1 μm (Eq. (2)) [35], where d is the volume (geometric) diameter of the particles and χ is the dynamic shape factor (equal to 1.0 for microspheres). d was obtained by visual imaging in SEM from the mean diameter of the particle size distribution of the aerogels expressed in a mass (or volume) basis.

$$d_{aero} = d \cdot \sqrt{\rho_{tapped}/\chi} \quad (2)$$

The particle size distribution of the gel precursors was obtained by visual imaging in an inverted optical microscope (IX51, Olympus, Tokyo, Japan). The zeta potential of these gels was measured by laser diffraction (Zetasizer Nano ZSP, Worcestershire, UK) in deionized water medium.

Attenuated total reflectance/Fourier-Transform Infrared Spectroscopy (ATR/FT-IR) was performed with a Gladi-ATR accessory using a diamond crystal (Pike, Madison, WI, USA). Raw salbutamol sulphate, raw sodium alginate, alginate aerogel microspheres and salbutamol sulphate-loaded alginate aerogel microspheres in the powdered form were characterized in the mid-IR spectrum range (400 – 4000 cm^{-1}) using 32 scans at a resolution of 2 cm^{-1}.

2.6 Salbutamol sulphate loading yield and release studies

Salbutamol content in the alcogels was indirectly measured by quantifying the SS content in the gelation medium after the ageing period and determined by difference with respect to the SS amount initially added. The absorbance of the aqueous solution was measured at 276 nm in a UV/Vis spectrophotometer (8453 equipment, Agilent, Santa Clara, CA, USA). Calibration curve of SS in water was obtained from triplicate dilution series, ranging from 0.02 to 0.17 mg/mL (R^2=0.9997).

Franz diffusion cells with a 6 mL-acceptor chamber were used to determine the release of SS from the alginate aerogel microspheres. Aerogel powder (3 mg) was evenly distributed on top of a cellulose membrane (0.45 µm pore size, Filter-Lab, Filtros Anoia, Barcelona, Spain) in the donor compartment. The diffusion area was 0.79 cm^2 (1 cm diameter). The receptor chamber was filled with PBS medium (pH 7.4 and 5.2) at 37ºC and constantly stirred at 100 rpm. Aliquots of 3 mL were sampled at certain time periods for 11 h and the volume replaced with fresh medium. SS concentrations in the aliquots were measured through UV/Vis spectrophotometry (8453 model, Agilent, USA) at 276 nm. Salbutamol content in the aerogels was measured by quantifying the SS content after 96 hours in the release medium. Calibration curve of SS in PBS was obtained from triplicate dilution series, ranging from 0.02 to 0.17 mg/mL (R^2>0.9999).

2.7 Simulated lung deposition tests

In vitro aerodynamic assessment of the SS-loaded aerogel particles was performed using a next generation impactor (NGI, Copley, Nottingham, UK) and a medium resistance single-dose dry powder inhaler (Plastiape Spa, Sirone, Italy) as device. The capsules size 3 (Coni-Snap, Capsugel, Colmar, France) were manually filled with 8.0 ± 0.2 mg of powder and the vacuum pump was activated at a flow of 60 L min^{-1} for 4.0 s to produce a pressure drop of 4 kPa, following the European Pharmacopeia guidelines. Prior to use, the seven collection stages of the impactor were coated with 1 % (w/v) solution of glycerin in methanol and then allowed to dry to prevent rebounding and to stabilize the particles. The terminal stage was a micro-orifice collector (MOC) covered with a glass fiber filter (Type A/E, Pall

Corporation, New York, NY, USA). SS was recovered from each stage of the impactor with appropriate volumes of a methanol:water 50:50 (v/v) solution, transferred into vials and drug concentrations measured by HPLC analysis. Stage 2 had a cut-off diameter of 4.46 μm. The aerodynamic performance of the formulation was evaluated from the emitted dose (ED; weight percentage of drug or powder exiting the device and entering the impactor), mass median aerodynamic diameter (d_{aero}; the particle diameter at 50% of the cumulative weight undersize) and fine particle fraction (FPF; mass of drug particles that have an aerodynamic diameter less than 5 μm related to the ED).

For the measurements of the SS content at each impactor stage, an HPLC equipment with an UV-detector (Agilent Technologies, Santa Clara, CA, USA) was used. The mobile phase consisted on PBS pH 7 and methanol (40:60 (v/v)) mixture at a rate of 0.6 mL/min, whereas the stationary phase was a Supelcosil™ LC-SCX column (250 mm x 4.6 mm, 5 μm) kept at 30ºC. 100 μL of sample were injected and the retention time was 13.3 min.

3. Results and Discussion

3.1 Gelation mechanism and processing window for alginate gel printing

Alginate is a polysaccharide excipient used in pharmaceutical formulations. Ionic gelation with divalent or trivalent cations, namely with Ca^{2+} cations, is the most common method of manufacture for alginate gels. These cations would form ionic bonds with the G-residues of the alginate polymeric chains in the so-called "*egg-box*" mechanism resulting in a gel of varying properties depending on the alginate source and cation-to-alginate content [36, 37]. Alginate gelation kinetics can be tuned by means of a prompt or modified release of the cations in the gelation bath. The diffusion method and internal setting method provide a sudden and modified (usually pH-controlled) release of Ca^{2+} cations, respectively. In this work, alginate picodroplets were jetted towards a $CaCl_2$ 0.5 M gelation bath to form the corresponding alginate gel microspheres using the internal setting gelation of alginate which is the only suitable method to preserve the spherical shape of the picodroplets in the gel form.

The processing window of alginate concentrations able to gelify in a bath of $CaCl_2$ 0.5 M aqueous solution was firstly determined by a standard prilling method. The choice of $CaCl_2$ as Ca^{2+} source is of particular interest since it is used as an excipient in dry powder formulations for pulmonary delivery (e.g., present in TOBI® Podhaler commercial product [12]). The

minimum alginate concentration leading to stable round gels was determined by prilling droplets of alginate solutions of decreasing concentrations starting at 1.5 % (w/w) and with steps of 0.25 % (w/w) from a syringe into the gelation bath. Following this method, the minimum alginate concentration was established at 0.25 % (w/w). The prilling method and modifications thereof (e.g., vibrating nozzle, jet cutting or spinning disks) can be useful in the preparation of monodisperse gel particles in the diameter range of hundreds of microns and above but fails to reach particle diameters below this threshold [38].

Thermal inkjet printing of alginate solutions is herein tested as a technique to obtain gel particles below 100 μm. However, the translation of the alginate gelation results from the prilling method into the thermal inkjet printing showed that the maximum feasible alginate concentration was limited by the jettability of the solution and directly linked to the viscosity of the propelled solution through the printhead. Higher concentrations of alginate in the aqueous solutions resulted in increased viscosities with the subsequent increase in the Reynolds number and Ohnesorge number of the jetted fluid [39]. Above a certain alginate concentration it will not be possible to print fluid. The maximum possible alginate concentration was set at 0.35 % (w/w), since 0.40 % (w/w) clogged the nozzles on multiple occasions. Overall, the feasible region for the printing of alginate gels was set at an alginate concentration of 0.25 to 0.35 % (w/w). After supercritical drying, the 0.35 % (w/w) provided the best results in terms of roundness and particle size homogeneity (Fig. 2), was used for further optimization.

FIGURE 2

3.2 Optimization of the alginate gel printing and solvent exchange process

The optimization of the printing method pursued the homogeneity of the particle sizes and an improvement in the sphericity of the particles. Moreover, the modifications of the process to be attempted should be compatible with the intended application of the aerogel carriers, mainly in terms of the mean particle size for the target administration route (inhalation) and of the drug loading yield (as high as possible).

The sphericity and homogeneity of the alginate microspheres obtained by inkjet printing was dramatically improved by using the same total gelation bath volumes (100 mL, Fig. 2c) but

splitted into four aliquots of 25 mL each (Fig. 3a). The replacement with fresh gelation baths was carried out after 30 printing cycles elapsed since the last bath replacement. The air-water contact surface of the gelation baths (i.e. the vessel internal diameter) and the distance between the printhead and the bath remained constant with respect to the previous attempts. The gel particles stayed at the top fluid layer of the gelation bath for a considerable period of time before settling. Thus, the probability of the jetted droplet of the alginate solution contacting an already formed gel particle on the water surface was lower in the case of the use of multiple gelation baths. As a result, the obtained particles were more spherical and showed less dimpled particles and less aggregation (Fig. 3a,c,d) with respect to the use of a single gelation bath (Fig. 2c). Gel particles showed a normal distribution with a mean value of 23.6±4.0 μm (in mass basis). Gels had a negative zeta potential (-4.4±0.4 mV) due to the negatively charged molecular chains of alginate that are partially compensated by the Ca^{2+} cations used for the gelation of the alginate [40].

The water contained in the alginate gel pores has low affinity for the extraction medium (i.e. supercritical CO_2) used for the supercritical drying. Therefore, water should be replaced by a compatible solvent before undergoing the drying step to prepare the aerogels. In this work, ethanol was used as solvent replacement since (a) it does not dissolve the gel structure, (b) is completely soluble with water, (c) is a poor solvent medium for the intended drug (salbutamol sulphate) to be loaded in the aerogel, and (d) is accepted as solvent for the manufacturing of pharmaceuticals. For alginate aerogel preparation [13, 26] as well as for other polysaccharides like chitosan [18] or κ-carrageenan [27], the sequential exchange of the gel solvent with aqueous solutions of increasing ethanol concentrations (*cf.* Section 2.3) prior to the supercritical drying may preserve better the structure of the wet gel in the resulting dry form (i.e. aerogel). However, the change of gel printing method to a five-step sequential solvent exchange resulted in a loss of particle sphericity and the appearance of dimples on the surface of the gel particles (Fig. 3b,e), likely due to the softening of the gels during the intermediate solvent exchange steps. Moreover, this solvent exchange procedure would likely reduce the loading yield of the drug, due to the partial solubility of salbutamol sulphate in water-ethanol mixtures.

FIGURE 3

Aerogel microspheres obtained through the optimized protocol (Fig. 3a) were in the form of free-flowing powder with a bulk density of 0.013 g/cm^3. The aerogel microspheres had a normal particle size distribution with a diameter of 23.8±4.5 μm, obtained by direct imaging and expressed as mean value ± standard deviation. The overall porosity of the particles was of 97.7% resulting in aerodynamic diameters of 2.4 μm, i.e. falling in the target size for effective lung deposition.

The aerogel particles presented a rough surface arising from the presence of surface pores in the nanometric range of mesopores and macropores according to the IUPAC classification (Fig. 4a,b). The voids between the intermingled fibrils of highly cross-linked alginate chains were mesoporous, whereas the voids between fibril bundles were macroporous. This mesoporous-to-macroporous contribution ratio was previously reported to be largely influenced by the alginate concentration in the precursor solution [41]. The porous distribution was homogeneous throughout the aerogel particles, since the inner structure of the particles observed by FIB-SEM (Fig. 4c,d) had a similar texture as the external one, but with slightly larger macropores (Fig. 4a,b).

The excellent textural properties of the optimized alginate aerogel particles were confirmed by nitrogen adsorption-desorption analysis (Table 1). Alginate aerogels had high BET-specific surface area (180 m^2/g) and BJH-specific pore volume (0.67 cm^3/g), whereas the mean pore diameter fell in the mesoporous range (17.8 nm). The values of these microspheres were lower than those obtained using the same printing technology by sequential solvent exchange and this fact was related to volume changes in the gels upon processing [13]. The same influence of the solvent exchange procedure on the textural properties was observed for the alginate aerogel beads (1.7 mm diameter) obtained by prilling techniques. The inkjet-printed particles showed lower BET-specific surface areas than their prilled granular counterparts, likely due to the higher external surface-to-volume ratio of the former ones. Overall, the textural properties of the printed aerogel microspheres seem promising to have enough loading capacity to host bioactive molecules for challenging their use as carriers for the pulmonary route.

FIGURE 4

Table 1. Specific surface area (A_{BET}), pore volume ($V_{p,BJH}$) and mean pore diameter ($d_{p,BJH}$) of alginate aerogel microspheres obtained by inkjet printing and followed by a direct or sequential (5 steps) solvent exchange to ethanol. The textural properties of alginate beads obtained by prilling of the same alginate stock solution and followed by the same solvent exchange protocols are also presented for the sake of comparison. Values are expressed as mean values ± standard deviation (n=3).

Gelation method	Solvent exchange	A_{BET} (m^2/g)	$V_{p,BJH}$ (cm^3/g)	$d_{p,BJH}$ (nm)
Inkjet	Direct	180±9	0.67±0.03	17.8±0.9
Inkjet	Sequential	397±20	1.48±0.07	14.4±0.7
Prilling	Direct	291±15	0.65±0.03	9.0±0.5
Prilling	Sequential	430±22	1.10±0.06	10.6±0.5

3.3 Salbutamol sulphate-loaded aerogels release study

SS-loaded aerogel microspheres were prepared by dissolving the bioactive agent in the gelation bath before the inkjet printing. This approach was taken to ensure a suitable loading of salbutamol in the gel since the SS is highly soluble in water (i.e. the gel solvent) and has a low solubility in absolute ethanol (i.e. the exchange gel solvent) [42]. After gelation, the content of SS in the printed gel particles was indirectly quantified as 7.8 % (w/w dried gel particle). After the subsequent solvent exchange and supercritical drying, a free-flowing powder was obtained with similar morphological and textural properties as the unloaded alginate aerogel microspheres (Fig. 5). The presence of SS in the alginate aerogel was confirmed by ATR/FT-IR analysis by the presence of a band at 1509 cm^{-1}, which is characteristic of the aromatic ring stretching mode of the drug molecule (Fig. S-1). The SS loading in the processed alginate aerogels was 3.0 % (w/w), a value compatible with the therapeutic salbutamol doses in commercially available dry powder inhalers (50-100 µg per dose).

FIGURE 5

The release of salbutamol sulphate from the aerogel matrix was recorded in diffusion Franz cells to mimic the air-liquid interface present in the lung and using a buffer solution (PBS) at pH 7.4 as simulated lung dissolution medium [43, 44]. A modified release profile was obtained for the drug contained in the aerogel microspheres (Fig. 6). Two steps can be distinguished in the release pattern: a sudden release during the first 15-30 min followed by a slow and sustained release of the remaining SS payload during a timeframe of 10 hours. The initial burst represents 10% of the total salbutamol contained in the aerogels. The drug fraction released during this step was attributed to the dissolution of weakly bound salbutamol, since the release rate was similar to the dissolution profile of the pure drug. A close observation to the external surface of the aerogels by SEM microscopy unveiled the presence of smooth needle-like salbutamol crystals (inset in Fig. 5), which was related to the drug fraction of the initial burst release. The formation of these crystals was attributed to the antisolvent effect of ethanol during the solvent exchange step, since similar crystal morphologies were obtained by antisolvent crystallization of SS aqueous solutions with ethanol [45].

The lungs contribute to the physiologic pH regulation through control of the partial pressure of CO_2. However, carbon dioxide production may exceed elimination in some acute episodes of asthma due to alveolar hypoventilation leading to respiratory acidosis (pH<7.4) [46]. Release of the salbutamol sulphate from the alginate matrix was tested at pH 5.2 and 7.4 with similar behavior due to the low variation of the ionic form fractions of the salbutamol sulphate (pK_a 9.3 and 10.3 [47]) and of the alginate (pK_a 1.5-3.5 [48]) in this pH range and the slow degradation of the matrix under these pH conditions [49].

Salbutamol sulphate used in dry powder inhalers as commercial products has a fast onset of action, featured by an action within 3-5 min after administration, with a peak after 15-20 min and duration of action of 4-6 hours. However, sustained release of $ß_2$-adrenergic agonists, particularly salbutamol, is also of therapeutic interest and is a current topic of research [50-52]. The salbutamol release profile obtained from the aerogels seems promising for the sustained release of this bronchodilator agent. The release profile can be of special interest to reduce the dosage administration frequency and side effects as well as to improve the patient compliance

for the treatment of chronic obstructive pulmonary disease, or to fit the patient rhythm in nighttime asthma treatments.

FIGURE 6

3.4 *In vitro* aerodynamic drug deposition of SS-loaded aerogels

The aerosol performance of the SS-loaded aerogels was evaluated from *in vitro* tests of the powder exiting the DPI device and entering an NGI impactor with 7 stages and a collector (Table 2 and Fig. 7). Due to the high porosity of the aerogels, the aerodynamic diameter obtained for the particles was *ca.* 6-fold lower than the aerogel particle size and in the respirable range (Table 2). The emitted dose as powder was close to 100% indicating the good flowability of the aerogel particles with reduced particle cohesion forces. The FPF values of the aerogels were close to 50 %, which means a better performance than other inkjet-printed (5-23 %) particles and some SS-commercial formulations (Cyclocaps®) [28, 29].

The SS deposition profile from the aerogel particles showed that the drug was mainly present in the first stage of the impactor (36.7 %) and the deposited drug contents gradually decreased from stage 1 to 7 (Fig. 7). The low drug contents in the last stages of the NGI impactor indicates that the local drug delivery will mainly take place at the bronchi and bronchioles.

Table 2. Aerodynamic properties of SS-loaded aerogel particles obtained by thermal inkjet printing followed by supercritical drying (n=3)

	SS-loaded aerogel
ED as powder (%)	97.5±1.2
ED as drug (%)	80.3±3.4
d_{aero} (μm)	4.0±1.5
FPF (%)	49.7±3.0

FIGURE 7

4. Conclusions

Particles manufactured by thermal inkjet printing and aerogel technology are endowed with unique nanostructure. Thermal inkjet printing prompted the engineering of reproducible and highly porous alginate-based microspheres. Process development unveiled a feasible printability region restricted by the polysaccharide concentration in the printable aqueous fluid. After supercritical drying of the alginate gels, aerogel microspheres in the form of free-flowing powder are obtained. The optimized formulation of the biopolymer aerogel particles has excellent and

homogenous textural properties falling in the nanoporous range. Moreover, the inkjet printing technique allows the reproducible gelation of spherical particles with narrow particle size distribution (23.8±4.5 μm). The processing technique is compatible with the incorporation of a bioactive compound (salbutamol sulphate) in the aerogel carrier for ulterior sustained release. The aerodynamic diameter of the drug-loaded printed aerogel particles is in the appropriate size range for lung deposition and local drug delivery. The material obtained by this innovative processing technique can be relevant for the treatment of several pulmonary diseases like asthma, chronic obstructive pulmonary disease or cystic fibrosis. This unique technology for printed aerogels can be extended to personalized medicine applications demanding nanostructured miniaturized and high-resolution product designs.

5. Acknowledgements

This work was supported by Xunta de Galicia [grant numbers ED431F 2016/010, ED431C 2016/008]; FEDER; MINECO [grant number SAF2017-83118-R]; Interreg V-A POCTEP Programme through FEDER funds from the European Union [grant numbers 0302_CVMAR_I_1_P, 0245_IBEROS_1_E]; and Agencia Estatal Investigación [AEI] of Spain. C.A. García-González acknowledges to MINECO for a Ramón y Cajal Fellowship [RYC2014-15239]. The authors would like to thank O'Toner Consumibles S.A. and the Technical Services Department of the USC for their valuable technical support with the selection and modifications of the inkjet cartridges and printer, respectively. Authors are also grateful to Dr. E. Solla (CACTI, Universidade de Vigo) for the technical support with the FIB-SEM images.

References

[1] G. Wang, Z. Wang, Z. Liu, J. Xue, G. Xin, Q. Yu, J. Lian, M.Y. Chen, Annealed graphene sheets decorated with silver nanoparticles for inkjet printing, Chem. Eng. J. 260 (2015) 582-589.

[2] W.J. Shin, H. Lee, Y. Sohn, W.G. Shin, Novel inkjet droplet method generating monodisperse hollow metal oxide micro-spheres, Chem. Eng. J. 292 (2016) 139-146.

[3] N. Scoutaris, S. Ross, D. Douroumis, Current Trends on Medical and Pharmaceutical Applications of Inkjet Printing Technology, Pharm. Res. 33 (2016) 1799-1816.

[4] R. Daly, T.S. Harrington, G.D. Martin, I.M. Hutchings, Inkjet printing for pharmaceutics – A review of research and manufacturing, Int. J. Pharm. 494 (2015) 554-567.

[5] E. Garreta, R. Oria, C. Tarantino, M. Pla-Roca, P. Prado, F. Fernández-Avilés, J.M. Campistol, J. Samitier, N. Montserrat, Tissue engineering by decellularization and 3D bioprinting, Mater. Today 20 (2017) 166-178.

[6] S.V. Murphy, A. Atala, 3D bioprinting of tissues and organs, Nat. Biotechnol. 32 (2014) 773-785.

[7] B.J. de Gans, P.C. Duineveld, U.S. Schubert, Inkjet Printing of Polymers: State of the Art and Future Developments, Adv. Mater. 16 (2004) 203-213.

[8] A.B.M. Buanz, C.C. Belaunde, N. Soutari, C. Tuleu, M.O. Gul, S. Gaisford, Ink-jet printing versus solvent casting to prepare oral films: Effect on mechanical properties and physical stability, Int. J. Pharm. 494 (2015) 611-618.

[9] A.B.M. Buanz, M.H. Saunders, A.W. Basit, S. Gaisford, Preparation of Personalized-dose Salbutamol Sulphate Oral Films with Thermal Ink-Jet Printing, Pharm. Res. 28 (2011) 2386-2392.

[10] J.H.Y. Chung, S. Naficy, G.G. Wallace, S. Naficy, S. O'Leary, Inkjet-Printed Alginate Microspheres as Additional Drug Carriers for Injectable Hydrogels, Adv. Polym. Tech. 35 (2016) 439-446.

[11] P.A. Meléndez, K.M. Kane, C.S. Ashvar, M. Albrecht, P.A. Smith, Thermal Inkjet Application in the Preparation of Oral Dosage Forms: Dispensing of Prednisolone Solutions and Polymorphic Characterization by Solid-State Spectroscopic Techniques, J. Pharm. Sci. 97 (2008) 2619-2636.

[12] A.M. Healy, M.I. Amaro, K.J. Paluch, L. Tajber, Dry powders for oral inhalation free of lactose carrier particles, Adv. Drug Deliver. Rev. 75 (2014) 32-52.

[13] C.A. García-González, M. Alnaief, I. Smirnova, Polysaccharide-based aerogels - Promising biodegradable carriers for drug delivery systems, Carbohydr. Polym. 86 (2011) 1425-1438.

[14] H. Maleki, L. Durães, C.A. García-González, P. del Gaudio, A. Portugal, M. Mahmoudi, Synthesis and biomedical applications of aerogels: Possibilities and challenges, Adv. Coll. Interface Sci. 236 (2016) 1-27.

[15] Z. Ulker, C. Erkey, An emerging platform for drug delivery: Aerogel based systems, J. Controll. Rel. 177 (2014) 51-63.

[16] M. Betz, C.A. García-González, R.P. Subrahmanyam, I. Smirnova, U. Kulozik, Preparation of novel whey protein-based aerogels as drug carriers for life science applications, J. Supercrit. Fluids 72 (2012) 111-119.

[17] C.A. García-González, E. Carenza, M. Zeng, I. Smirnova, A. Roig, Design of biocompatible magnetic pectin aerogel monoliths and microspheres, RSC Adv. 2 (2012) 9816-9823.

[18] H. Kayser, C.R. Müller, C.A. García-González, I. Smirnova, W. Leitner, P. Domínguez De María, Dried chitosan-gels as organocatalysts for the production of biomass-derived platform chemicals, Appl. Catal. A: General 445-446 (2012) 180-186.

[19] S. Zhao, W.J. Malfait, N. Guerrero Alburquerque, M.M. Koebel, G. Nyström, Biopolymer Aerogels and Foams: Chemistry, Properties and Applications, Angew. Chem. Int. Ed. 57 (2018) 7580-7608.

[20] I. Smirnova, P. Gurikov, Aerogels in Chemical Engineering: Strategies Toward Tailor-Made Aerogels, Annu. Rev. Chem. Biomolec. Eng. 8 (2017) 307-334.

[21] A. Tripathi, G.N. Parsons, S.A. Khan, O.J. Rojas, Synthesis of organic aerogels with tailorable morphology and strength by controlled solvent swelling following Hansen solubility, Sci. Rep. 8 (2018) 2106.

[22] S.M. Jung, H.Y. Jung, M.S. Dresselhaus, Y.J. Jung, J. Kong, A facile route for 3D aerogels from nanostructured 1D and 2D materials, Sci. Rep. 2 (2012) 849.

[23] F. De Cicco, P. Russo, E. Reverchon, C.A. García-González, R.P. Aquino, P. Del Gaudio, Prilling and supercritical drying: A successful duo to produce core-shell polysaccharide aerogel beads for wound healing, Carbohydr. Polym. 147 (2016) 482-489.

[24] M. Pinnow, H.-P. Fink, C. Fanter, J. Kunze, Characterization of Highly Porous Materials from Cellulose Carbamate, Macromol. Symp. 262 (2008) 129-139.

[25] K.P. Lee, G.L. Gould, Aerogel powder therapeutic agents, 2006, US Patent US6994842(B2)

[26] M. Alnaief, M.A. Alzaitoun, C.A. García-González, I. Smirnova, Preparation of biodegradable nanoporous microspherical aerogel based on alginate, Carbohydr. Polym. 84 (2011) 1011-1018.

[27] M. Alnaief, R. Obaidat, H. Mashaqbeh, Effect of processing parameters on preparation of carrageenan aerogel microparticles, Carbohydr. Polym. 180 (2018) 264-275.

[28] W. Mueannoom, A. Srisongphan, K.M.G. Taylor, S. Hauschild, S. Gaisford, Thermal ink-jet spray freeze-drying for preparation of excipient-free salbutamol sulphate for inhalation, Eur. J. Pharm. Biopharm. 80 (2012) 149-155.

[29] G. Sharma, W. Mueannoom, A.B.M. Buanz, K.M.G. Taylor, S. Gaisford, In vitro characterisation of terbutaline sulphate particles prepared by thermal ink-jet spray freeze drying, Int. J. Pharm. 447 (2013) 165-170.

[30] B.A. García-Torres, A. Aguilar-Elguezabal, M. Román-Aguirre, L. Álvarez-Contreras, Synthesis of silica aerogels microspheres prepared by ink jet printing and dried at ambient pressure without surface hydrophobization, Mater. Chem. and Phys. 172 (2016) 32-38.

[31] M. Walshaw, G. McElvaney, R. Williams, A. Morice, M. Carroll, C. Haworth, M. Herzig, I. Ketchell, R. Myrvold, N. Meland, A.H. Myrset, K.T. Smerud, A first-in-patient clinical trial demonstrates that inhaled alginate oligosaccharide (OligoG) is well tolerated in cystic fibrosis (CF) patients, J. Cys. Fibros. 13 (2014) S58.

[32] M.F. Pritchard, L.C. Powell, A.A. Jack, K. Powell, K. Beck, H. Florance, J. Forton, P.D. Rye, A. Dessen, K.E. Hill, D.W. Thomas, A low molecular weight alginate oligosaccharide disrupts pseudomonal microcolony formation and enhances antibiotic effectiveness, Antimicrob. Agents Ch. 61 (2017) e00762.

[33] L. Goimil, M.E.M. Braga, A.M.A. Dias, J.L. Gómez-Amoza, A. Concheiro, C. Alvarez-Lorenzo, H.C. de Sousa, C.A. García-González, Supercritical processing of starch aerogels and

aerogel-loaded poly(ε-caprolactone) scaffolds for sustained release of ketoprofen for bone regeneration, J. CO2 Utiliz. 18 (2017) 237-249.

[34] D. Wu, C. Wang, J. Yang, H. Wang, H. Han, A. Zhang, Y. Yang, Q. Li, Improving the Intracellular Drug Concentration in Lung Cancer Treatment through the Codelivery of Doxorubicin and miR-519c Mediated by Porous PLGA Microparticle, Molec. Pharm. 13 (2016) 3925-3933.

[35] A.J. Hickey, D.A. Edwards, Density and Shape Factor Terms in Stokes' Equation for Aerodynamic Behavior of Aerosols, J. Pharm. Sci. 107 (2018) 794-796.

[36] P. Gurikov, I. Smirnova, Non-Conventional Methods for Gelation of Alginate, Gels 4 (2018) 14.

[37] K.Y. Lee, D.J. Mooney, Alginate: Properties and biomedical applications, Prog. Polym. Sci. 37 (2012) 106-126.

[38] M. Mishra, Handbook of Encapsulation and Controlled Release, CRC Press2015.

[39] G.H. McKinley, M. Renardy, Wolfgang von Ohnesorge, Phys. Fluids 23 (2011) 127101.

[40] D. Kaneko, N.Q. Thi le, T. Shimoda, T. Kaneko, Preparation methods of alginate micro-hydrogel particles and evaluation of their electrophoresis behavior for possible electronic paper ink application, Polym. J. 42 (2010) 829-833.

[41] A. Veronovski, Ž. Knez, Z. Novak, Preparation of multi-membrane alginate aerogels used for drug delivery, J. Supercrit. Fluids 79 (2013) 209-215.

[42] H.S.M. Ali, P. York, N. Blagden, M. Khoubnasabjafari, W.E. Acree, A. Jouyban, Solubility of salbutamol and salbutamol sulphate in ethanol+water mixtures at 25°C, J. Mol. Liq. 173 (2012) 62-65.

[43] S. May, B. Jensen, M. Wolkenhauer, M. Schneider, C.M. Lehr, Dissolution Techniques for In Vitro Testing of Dry Powders for Inhalation, Pharm. Res. 29 (2012) 2157-2166.

[44] K. Shah, L.W. Chan, T.W. Wong, Critical physicochemical and biological attributes of nanoemulsions for pulmonary delivery of rifampicin by nebulization technique in tuberculosis treatment, Drug Deliv. 24 (2017) 1631-1647.

[45] M.J. Davies, T.D. Kerry, L. Seton, M.F. Murphy, P. Gibbons, J. Khoo, M. Naderi, The crystal engineering of salbutamol sulphate via simulated pulmonary surfactant monolayers, Int. J. Pharm. 446 (2013) 34-45.

[46] R.A. Johnson, A Quick Reference on Respiratory Acidosis, Vet. Clin. North Am. Small Anim. Pract. 47 (2017) 185-189.

[47] V.B. Sutariya, R.C. Mashru, M.G. Sankalia, J.M. Sankalia, Transbuccal delivery of salbutamol sulphate: In vitro determination of routes of buccal transport, Ars Pharm. 46 (2005) 337-352.

[48] C.A. García-González, M. Jin, J. Gerth, C. Alvarez-Lorenzo, I. Smirnova, Polysaccharide-based aerogel microspheres for oral drug delivery, Carbohydr. Polymers 117 (2015) 797-806.

[49] V. Guarino, T. Caputo, R. Altobelli, L. Ambrosio, Degradation properties and metabolic activity of alginate and chitosan polyelectrolytes for drug delivery and tissue engineering applications, AIMS Mater. Sci. 2 (2015) 497-502.

[50] C. Kumaresan, K. Sathishkumar, Development of an Inhaled Sustained Release Dry Powder Formulation of Salbutamol Sulphate, an Antiasthmatic Drug, Indian J. Pharm. Sci. 78 (2016) 136-142.

[51] F.M. Ducharme, M. Ni Chroinin, I. Greenstone, T.J. Lasserson, Addition of long-acting beta2-agonists to inhaled corticosteroids versus same dose inhaled corticosteroids for chronic asthma in adults and children, Cochrane Database Syst. Rev. 5 (2010) CD005535.

[52] Q. Li, S. Zhan, Q. Liu, H. Su, X. Dai, H. Wang, H. Beng, W. Tan, Preparation of a Sustained-Release Nebulized Aerosol of R-terbutaline Hydrochloride Liposome and Evaluation of Its Anti-asthmatic Effects via Pulmonary Delivery in Guinea Pigs, AAPS PharmSciTech 19 (2018) 232-241.

Figure captions

Figure 1. Setup used for the preparation of the alginate gel microspheres. The inkjet printer (1) is connected to a computer (2) that allows the control of the printing operation by the heating element (3) of the cartridge and controls the x-axis movement of the printer belt (4). The printer is located in a metallic support with moving parts allowing its y-axis control (i.e. the printhead-

to-gelation bath distance). The alginate solution is located in the printhead (5) containing several printing chambers. An electrical signal is applied to a micro-thermal heater (6) located at each printing chamber, and the sudden increase in the temperature generates a vapor bubble (7) that ejects the alginate solution as a picodroplet (8) through the nozzle (9). The droplets are jetted to a gelation bath (10) constantly agitated with a magnetic stirrer (11).

Figure 2. SEM images of alginate aerogel microparticles obtained from preliminary inkjet printing trials from alginate aqueous solutions of different concentrations: (a) 0.25, (b) 0.30, (c) 0.35, and (d) 0.40 % (w/w). A single gelation bath of 100 mL of $CaCl_2$ 0.5 M and a direct solvent exchange to ethanol was used in all cases. Printhead clogging events occurred when using the 0.40 % (w/w) alginate solution.

Figure 3. SEM images of alginate aerogel microparticles obtained by inkjet printing of 10 mL of 0.35 % (w/w) alginate aqueous solutions into multiple gelation baths of 25 mL of $CaCl_2$ 0.5 M with (a) direct or (b) sequential solvent exchange to ethanol. (c,d) Loosely aggregated and spherical particles were obtained using the direct solvent exchange, (e) whereas the sequential solvent exchange resulted in the presence of dimples in the particle surface (white arrow).

Figure 4. Morphological and textural characterization of the alginate aerogel microspheres obtained through the optimized conditions for the printing protocol: External (a) morphology and (b) nanostructure obtained by SEM microscopy; and internal (c) cross section and (d) nanostructure obtained by FIB-SEM microscopy.

Figure 5. SEM image of the porous surface of printed alginate aerogel particles loaded with 3 % (w/w) of salbutamol sulphate. Inset: higher magnification of the surface showing a fraction of the drug in the form of needle-like crystals.

Figure 6. *In vitro* release profile of SS from alginate aerogel micropheres (white circles) in PBS pH 7.4 solution (37°C, 100 rpm). The dissolution profile of SS (black squares) under the same operating conditions is plotted for the sake of comparison.

Figure 7. Drug deposition profile of salbutamol sulfate loaded in alginate aerogel particles with an NGI impactor (n=3, mean ± standard deviation).

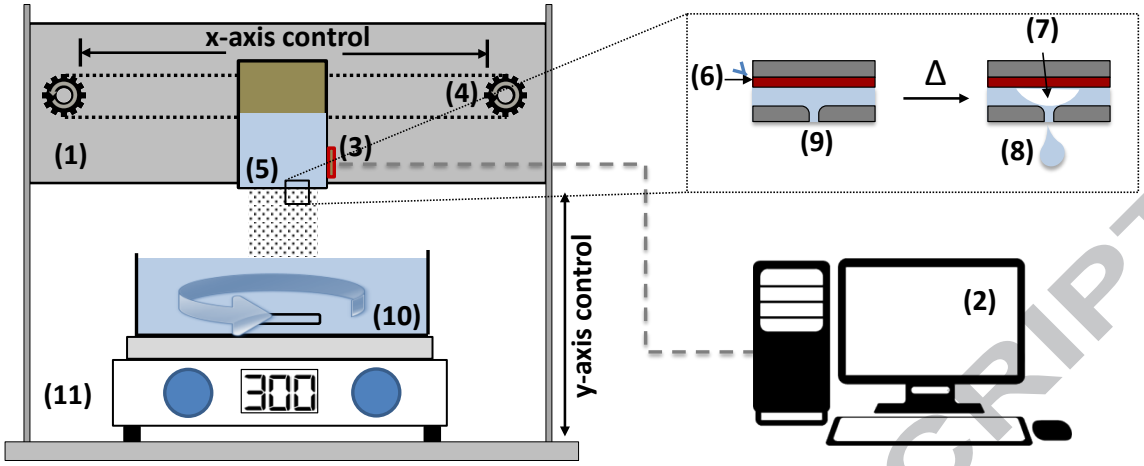

FIGURE 1

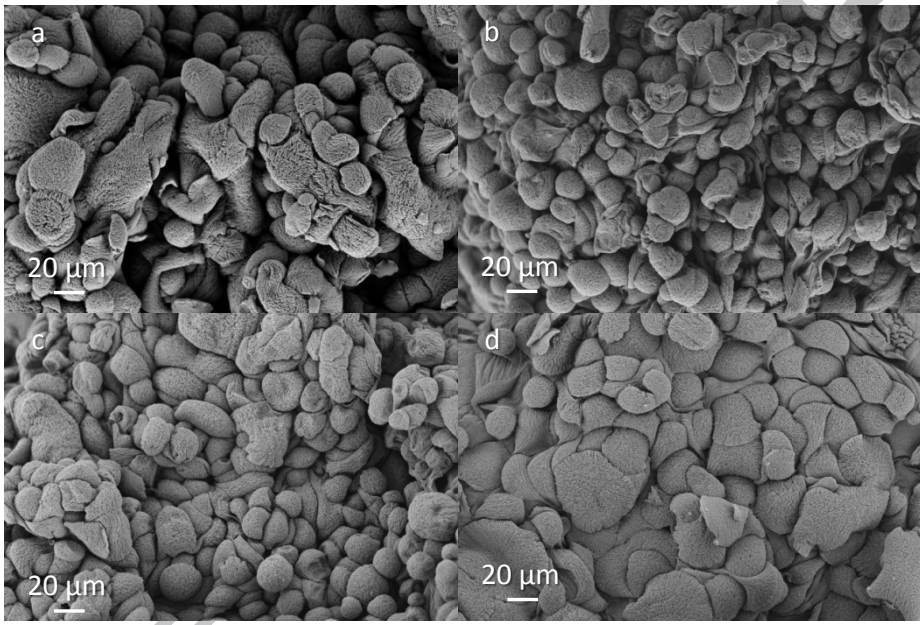

FIGURE 2

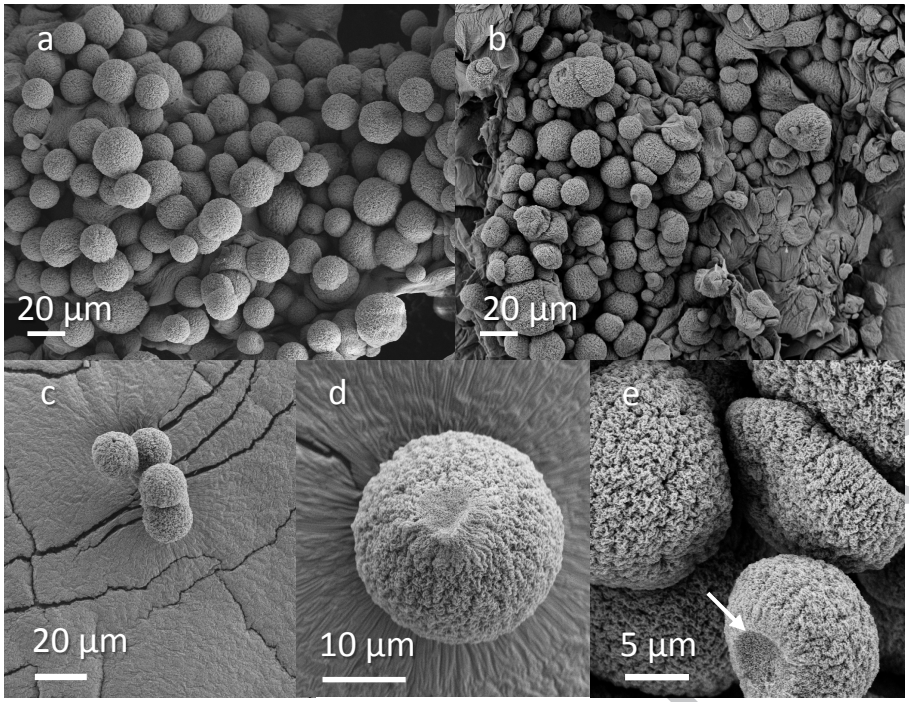

FIGURE 3

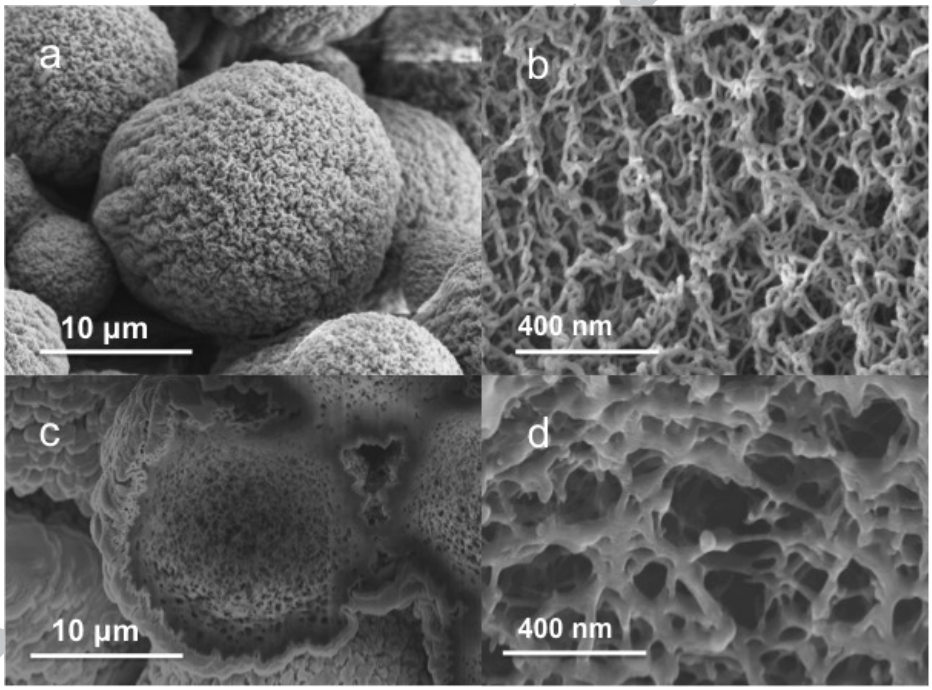

FIGURE 4

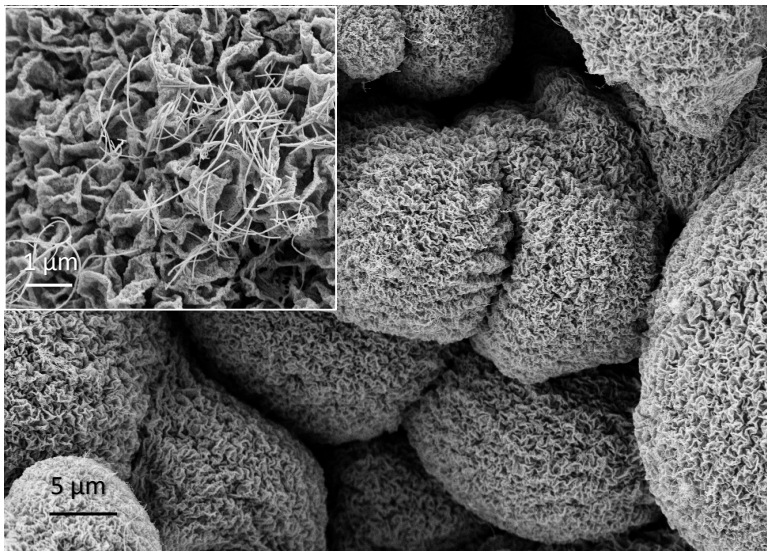

FIGURE 5

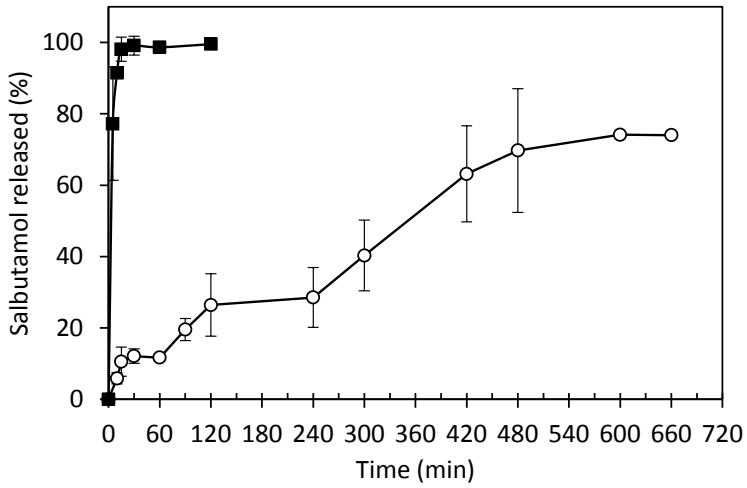

FIGURE 6

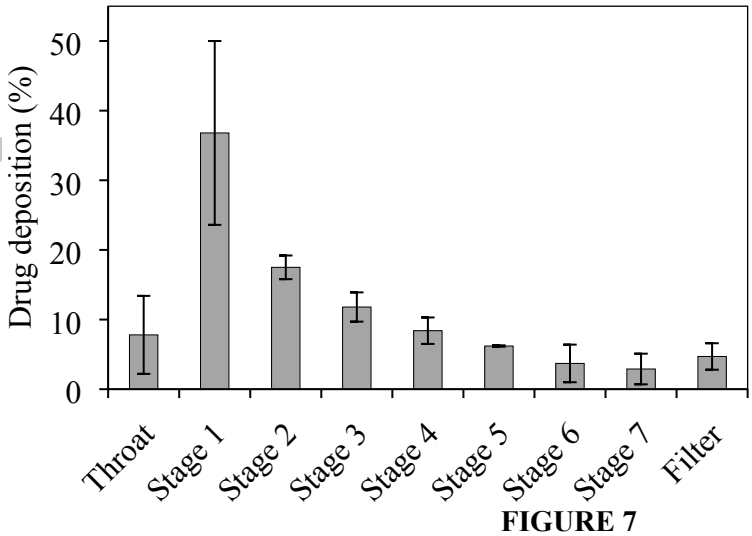

FIGURE 7

Graphical abstract

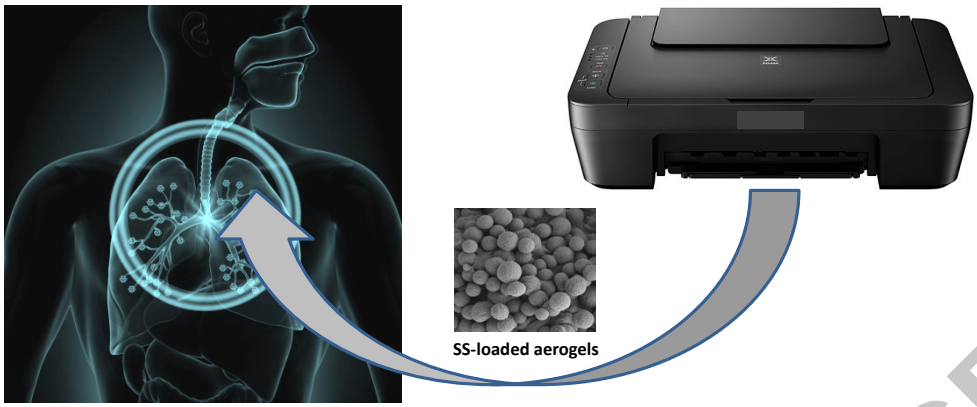

Highlights:

- Aerogels are prepared by thermal inkjet printing followed by supercritical drying
- Process has a printability region restricted by the gel precursor concentration
- Aerogel microspheres have narrow size distribution and high textural properties
- The processing technique is compatible with incorporation of bioactive compounds
- Aerogels are relevant for pulmonary administration and for personalized medicine